Biomechanical assessment and fatigue characteristics of an articulating nucleus implant

Nathaniel R. Ordway, William F. Lavelle, Tim Brown and Q-Bin Bao

Int J Spine Surg 2013, 7 () e109-e117
doi: https://doi.org/10.1016/j.ijsp.2013.10.001
https://www.ijssurgery.com/content/7/e109

The International Journal of Spine Surgery
2397 Waterbury Circle, Suite 1,
Aurora, IL 60504, Phone: +1-630-375-1432

Available online at www.sciencedirect.com

ScienceDirect

International Journal of Spine Surgery 7 (2013) e109–e117

INTERNATIONAL SOCIETY for the ADVANCEMENT of SPINE SURGERY
www.sasjournal.com

Biomechanical assessment and fatigue characteristics of an articulating nucleus implant

Nathaniel R. Ordway, MS[a,*], William F. Lavelle, MD[a], Tim Brown, MS[b], Q-Bin Bao, PhD[c]

[a] *Department of Orthopedic Surgery, SUNY Upstate Medical University, Syracuse, NY*
[b] *Pioneer Surgical Technology, Marquette, MI*
[c] *Bonovo Orthopedics, Beijing, P R China*

Abstract

Background: Extrusion is a known complication of lumbar nucleus replacement devices. Despite this fact, this complication has not been well studied in an in vitro cadaveric model under fatigue-loading conditions.
Methods: Lumbar constructs (with treated and control levels) were tested in intact, postdisectomy, and postnucleus implant conditions under compression, torsion, and bending for initial biomechanical assessment. Constructs were then tested for 100(k) cycles under fatigue loading to assess extrusion risk. Potential adverse effects to vertebral and endplate fractures were assessed using gross dissection and macroscopic and micro-computed tomography evaluation techniques.
Results: Based on the initial biomechanical assessment, implantation of the nucleus device significantly increased disc height compared with the discectomy condition, and there were no significant differences between the intact and implanted conditions for range of motion or stiffness. All constructs completed the 100(k) cycles with no extrusions. There was evidence of implant shift toward the right lateral annulus on postfatigue images. Postfatigue dissection and imaging showed no evidence of macroscopic endplate or trabecular fractures.
Conclusion: Using a 2-level lumbar in vitro construct, the biomechanical function of the treated level with an articulating nucleus implant was similar to intact. In vitro fatigue testing showed no implant extrusion and macroscopic changes to the bony structure or cartilaginous endplates when comparing treated and intact levels.

Keywords: Lumbar spine; Intervertebral disc; Nucleus replacement; Disc height; Lateral bending; Range of motion

Introduction

In industrialized nations, back pain is nearly ubiquitous with a prevalence of 60%–90%, which is second only to the common cold as a reason for a physician visit.[1] Although it is extremely difficult to accurately identify a pain generator, disc degeneration is postulated to be the common and often times the earliest precipitator of low-back pain. With regard to spinal mechanics, discs act to bear and distribute loads as well as dissipate energy.[2] The ability of the disc to perform these functions is primarily attributed to its unique composition of the soft proteoglycan-rich inner core (nucleus pulposus) and the tough collagen-rich outer shell (annulus fibrosus).[2–5]

Disc degeneration in general results from reduced proteoglycan content in the nucleus and reduced nuclear hydration. The resulting biomechanical changes in the disc lead to loss of disc height and increasing biomechanical demand on the annulus with imbalance in the stress distribution across the disc space.[5,6] As tension in the annulus is lost, an anterior or posterior instability of the motion segment can ensue. Increasing loads on the annulus may lead to annular tears with or without disc herniations. Continued loss of disc height can lead to osteophyte formation, facet arthrosis, and stiffness of the motion segment. Pain from degenerative disc disease (DDD) occurs at any stage of this degenerative cascade from very early disc degeneration to instability and deformity.

Traditional treatment modalities for symptoms resulting from disc degeneration are focused on decompression with or without fusion. These treatment modalities do not attempt to halt the degenerative cascade, and in many instances, lead to further progression of degeneration. Although short-term outcomes after lumbar discectomy have been shown to be superior to conservative care,

* Corresponding author: Nathaniel R. Ordway, MS, Department of Orthopedic Surgery, SUNY Upstate Medical University, 750 East Adams St, Syracuse, NY 13210; Tel.: +1-315-464-6462; fax: +1-315-464-6638
E-mail address: ordwayn@upstate.edu

2211-4599
http://dx.doi.org/10.1016/j.ijsp.2013.10.001

long-term outcomes have been compromised by persistent back pain and a high risk of reoperations with a significant number of reherniations.[7–10] Arthrodesis of the motion segment is still the gold standard for treatment of chronic disabling back pain of discogenic origin. However, it is difficult to predict the clinical response to arthrodesis as it depends on multiple factors, such as, the diagnosis, previous surgeries, prior fusion attempts, and number of levels requiring fusion. Long-term studies have shown a fusion rate of 87% and clinical success rate of 76% for DDD.[11,12] There are several disadvantages inherent to arthrodesis; most importantly, it can change the biomechanical loading of the adjacent segment leading to accelerated degeneration.[13,14]

In this context, intradiscal replacement of the nucleus is one possible alternative to spinal fusion procedures and the procedure has a history.[15,16] While preserving the biomechanics of the annulus fibrosus and cartilaginous endplate, nucleus pulposus implants are designed to provide stable motion, increase disc space height, relieve or lessen transmission of shear forces on the remaining annulus (restoring their natural length), and stabilize spinal ligamentous structures.[3] Currently, the indication for a nucleus replacement is for symptomatic lumbar discogenic back pain not responding to active conservative treatment for a minimum of 6 months. An magnetic resonance imaging should demonstrate early-stage degenerative changes with disc height more than 5 mm and an absence of Schmorl nodes. Standing X-rays should also demonstrate spondylolisthesis less than grade I at the symptomatic level, with disc height loss less than 50%.[14,17]

Nucleus replacement with a variety of prosthetic materials has been described. The success of such devices has been limited.[18–21] Unfortunately, a commonly reported complication has been extrusion of the device from the intradiscal space.[21–24] Various reasons for device extrusion have been demonstrated. These range from failure of the annular injury to heal, to the use of undersized devices, to fragmentation of the device itself. Potential patients for a device like a nuclear replacement are typically in the second to fourth decade of life. Arthroplasty devices for such patients will need to reliably last 30–40 years. Both the history of device failure and the lengthy service life of a nuclear replacement mandate rigorous biomedical fatigue testing to ensure patient safety and satisfaction. Fatigue testing of individual devices under physiologic loads for millions of cycles is possible if the goal is to examine the wear and longevity of the device itself.[20,25,26] However, the commonly reported problem for these devices relates to extrusion from the intervertebral disc space and the best available model is an in vitro cadaveric model.[20,27,28]

The purpose of this study was to assess the biomechanical function of an articulating nucleus replacement device in an in vitro cadaveric model and assess any adverse effects on the intervertebral disc and vertebral endplate under fatigue-loading conditions. More specifically, this was a preclinical pilot study examining an unconstrained polyetheretherketone (PEEK) on PEEK nucleus replacement (Nubac, Pioneer Surgical Technology, Marquette, Michigan). This device was designed to have an internal articulation and 2 smooth endplates and therefore allows limited translation within the intervertebral disc space (Fig. 1).

Materials and methods

Specimen preparation

Three fresh-frozen human cadaver spines from the 12th thoracic vertebrae through the sacrum were harvested and stored at −20°C until testing. Each specimen underwent plain X-ray in anteroposterior (AP) and lateral views and a lumbar dual-energy X-ray absorptiometry scan to assess the disc height, osteophyte formation, and bone density. The lumbar dual-energy X-ray absorptiometry followed a standardized lumbar spine clinical protocol (GE Lunar DPX-IQ), and scanning was performed with rice bags surrounding each specimen to emulate the abdominal tissues. Exclusion criteria consisted of significant disc height loss (disc height less than 7 mm), significant osteophyte formation, or evidence of osteoporosis (T score less than −2.5 or for this age and gender bone density less than 0.76 g/cm^2). Table 1 lists the specimen information.

Test specimens consisted of a contiguous pair of functional spinal units (FSUs), which resulted in 2 specimens per spine (T12-L2 and L3-5). For each specimen, 1 intervertebral disc served as a control level (randomized) and the adjacent intervertebral disc served as a surgical level (treatment).

Nondestructive biomechanical tests

The top and bottom vertebral bodies of the specimen were potted into fixtures and attached to a servohydraulic materials testing machine (MTS Corp, Eden Praire,

Fig. 1. Articulating PEEK nucleus replacement used in this study.

Table 1
Specimen information (N = 6)

Specimen	Gender	Age	BMD (g/cm^3)	Disc depth (cm)	Disc width (cm)	Disc area (cm^2)	Percenatge of implant/disc area
7761 (T12-L2)	M	54	1.538	4.11	5.43	17.84	10.65
7761 (L3-5)	M	54	1.538	4.07	6.37	20.02	9.49
7827 (T12-L2)	M	58	0.786	3.79	5.21	15.53	15.52
7827 (L3-5)	M	58	0.786	3.98	5.36	17.57	13.72
7760 (T12-L2)	M	65	0.919	3.73	5.45	16.99	14.18
7760 (L3-5)	M	65	0.919	3.74	5.43	16.51	14.60
Mean		59	1.081	3.90	5.54	17.41	13.03
St. dev.		5	0.359	0.17	0.42	1.52	2.39

Abbreviations: BMD, bone mineral density; St. dev., standard deviation.

Minnesota) for the testing. Tilt sensors (Crossbow Technology, Inc, San Jose, California) were attached to each fixture and to the middle vertebral body of each specimen to collect angular motion data of individual levels in the sagittal and coronal planes. The initial MTS actuator displacement (axial and torsional) for each FSU was captured under a static 10 N of compressive load and before any loading (baseline value). This baseline represented the initial specimen height and rotation. A battery of loading modes was applied. The loading modes were compression, flexion compression, extension compression, lateral bending compression (right and left), and torsion (right and left). Preconditioning was performed in each loading mode by applying 5 ramp loading cycles and then data were collected by ramp subsequent loading cycles. The loading rate for all 10 cycles was 0.05 Hz. The applied load, displacement, and the angle of each tilt sensor were monitored using a PC-based data acquisition system with a sampling rate of 10 Hz. A peak load of 1200 N was applied for the compression test and a peak moment of 7.5 Nm was applied for the flexion-, extension-, bending-, and torsion-loading modes. For flexion, extension, and lateral bending test modes, the maximum applied load was 500 N at an offset of 15 mm and represented applied bending moments. During the testing period, the specimens were tested at room temperature and wrapped in saline-soaked gauze to prevent dehydration.

Surgical discectomy

A discectomy was performed on the designated implant level using a right lateral approach and standard surgical instruments. An annular incision (box cut) of approximately 6 × 10 mm was made using a surgical scalpel. The surgical discectomy involved creating a complete nucleotomy with rongeurs. The location and width of the cavity was checked by placing the rongeur in the cavity against the far wall of the annulus and taking an AP image with a C-arm (Fluoroscan Imaging Systems, Bedford, Massachusetts). This was performed to confirm that the cavity was centrally located for implant placement. Discectomy was continued until a central location of the cavity was confirmed. Following the discectomy procedure, the same nondestructive biomechanical testing, as aforementioned, was repeated.

Nucleus replacement

A trial spacer was inserted into the disc space to determine implant size. Based on feel, if the trial spacer was loose in the disc space after the insertion, the trial was

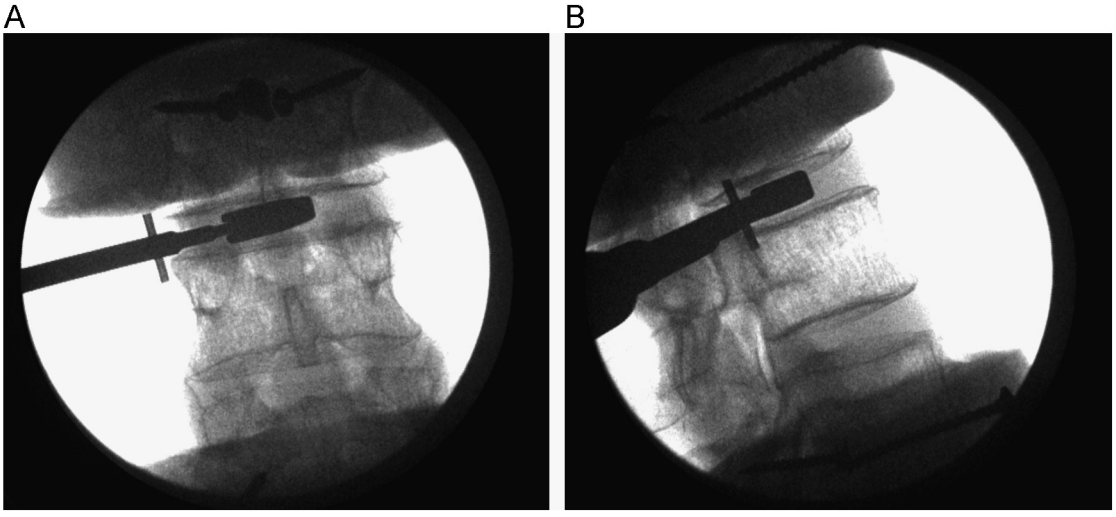

Fig. 2. Radiographic image of trial spacer for sizing of the nucleus implant in (A) AP and (B) lateral views.

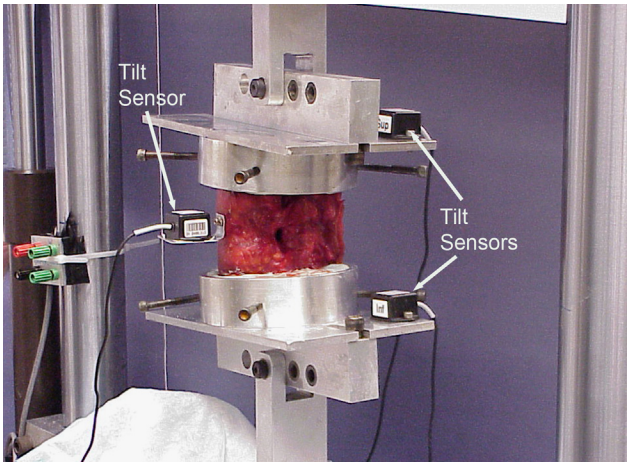

Fig. 3. Biomechanical test setup of an example test specimen in left lateral bending before fatigue test protocol.

removed and a larger trial was inserted. The process was repeated until the trial was snug in the disc space without excessive distraction (Fig. 2). An appropriate size-matched implant was inserted and centrally positioned. Confirmation of a central location was provided using AP and lateral images acquired by the C-arm. The nondestructive biomechanical testing was conducted for a third time.

Fatigue test

A fatigue test followed, which was conducted in left lateral bending mode (Fig. 3). The load ranged from 2.5–7.5 Nm (a compressive 250–750 N load offset 10 mm), and the test was run at 2 Hz for 100,000 cycles. The left lateral bending mode represented a "worst-case" scenario with regard to implant extrusion by the load being applied opposite of the annular incision site. During the fatigue test, the exposed specimen was wrapped in saline-soaked gauze and parafilm for approximately 14 hours of testing to prevent dehydration.

Specimen dissection

Upon completion of the mechanical tests, each specimen underwent radiography and was examined for possible fractures or migration or both. Intervertebral discs were dissected transversely through the midplane of the disc space. Both the intact and implanted discs were examined macroscopically for potential changes. Photographs of the disc were taken using a macro lens to document the condition of the disc space (Fig. 4). For the implanted levels, implant position, as well as cavity size and shape, was noted. The cross-sectional area, width, and depth of the disc were determined utilizing ImagePro software (Media Cybernetics, Inc, Silverspring, Maryland). The contact area of the implant with the endplates was also measured. Disc tissue was dissected to visually examine the endplates of the control and implanted levels for macroscopic fractures.

Microfracture evaluation

The L1 and L4 vertebral bodies were dissected and scanned on a μCT 80 (Scanco Medical AG, Bassersdorf, Switzerland) to examine the endplates and underlying trabecular bone for potential fractures. The specimens were scanned with an X-ray energy of 70 kVp and current of 114 mA and an isotropic voxel resolution of 74 m (image matrix of 1024 × 1024). A total of 500 projections over 180° were collected for each vertebra. An integration time of 700 ms per projection was used, which resulted in a scan time of about 2.5–3 hours per specimen. The slice thickness was 0.5 mm. Images were then sent to a core laboratory (Medical Metrics, Inc) for radiographic evaluation by a board-certified, fellowship-trained, practicing radiologist. For each vertebra, 1 endplate was representative of the control level and the other endplate was representative of the implanted level.

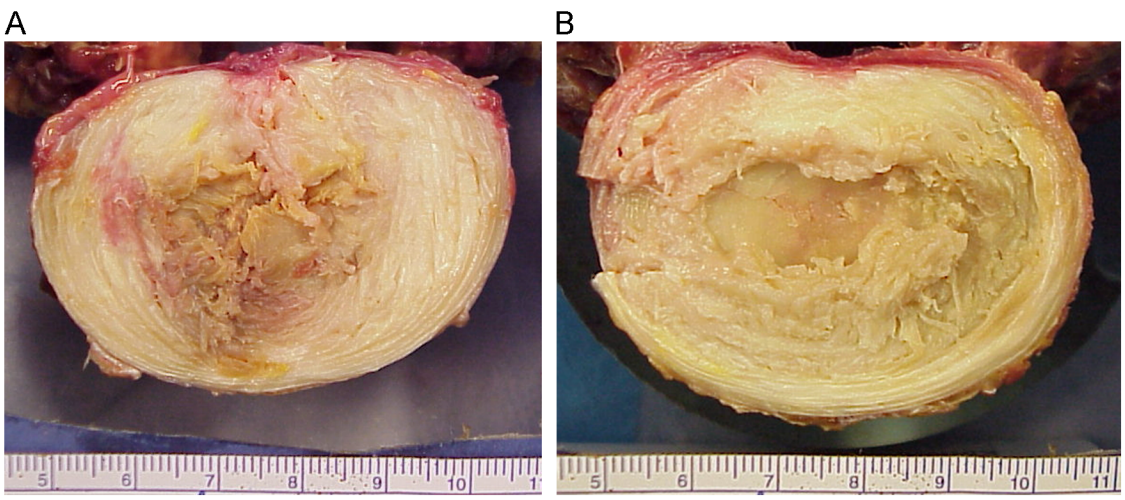

Fig. 4. Macroscopic cross-section of the intervertebral disc following fatigue testing of 100(k) cycles for (A) an intact, untreated disc and (B) an implanted disc.

Data and statistical analysis

The digital data collected during the biomechanical tests were analyzed using an algorithm developed in LabView (National Instruments, Austin, Texas). The applied load versus displacement (or moment vs angle) curves were used to calculate the range of motion (ROM) and stiffness for the battery of loading modes in each condition (intact, post-discectomy, and postimplant). The ROM in compression was determined for the 2-level specimen and was based on the change in displacement from the initial specimen height and the specimen height at 1.2 kN of the fifth cycle. For torsion, the ROM was determined for the 2-level specimen and was based on the change in angular motion from the initial specimen rotation and the specimen rotation at 7.5 Nm of the fifth cycle. The ROM in each of the bending-loading modes (flexion and extension and left and right bending) was determined by the angle recorded at the peak load of the fifth cycle. The stiffness was determined from a linear portion of the curve (0.8 kN–1.2 kN compression and 2.5–7.5 Nm for all others) for the last 3 cycles of testing and was then averaged. A repeated-measures analysis of variance was used to examine differences in ROM and stiffness with specimen condition (intact, discectomy, and implanted) as the main factor. Where appropriate, post hoc Student's t tests were performed to compare control and surgical levels. A significance level of $\alpha = 0.05$ was set for all comparisons.

Implant extrusion and fractures to the vertebrae as a result of the fatigue testing were assessed qualitatively. Implant extrusion was assessed by direct observation during fatigue testing, and positioning of the implant within the disc cavity was assessed after fatigue testing following disc dissection. Gross macroscopic fractures were determined from the radiographs obtained after fatigue testing, and dissection for both the control and surgical levels were also assessed. The existence of microfractures was assessed by visually inspecting the micro-computed tomography (CT) images by a board-certified, fellowship-trained, practicing radiologist.

Results

Nondestructive biomechanical tests

The change in specimen (disc) height was monitored during pure compression for the various disc conditions. Fig. 5 displays the mean loss in disc height for the 3 conditions tested. The disc height after discectomy significantly decreased ($P < .05$) in comparison with the intact condition under 1.2 kN of compressive loading. Implantation of the nucleus device significantly increased ($P < .05$) the disc height compared with the discectomy condition. There was no significant difference between the intact and implanted conditions. The amount of torsional rotation was measured for both left and right torsion at 7.5 Nm on the fifth cycle. Table 2 lists the mean torsional rotation for the various disc conditions. There were no significant differences in torsional motion for any disc condition.

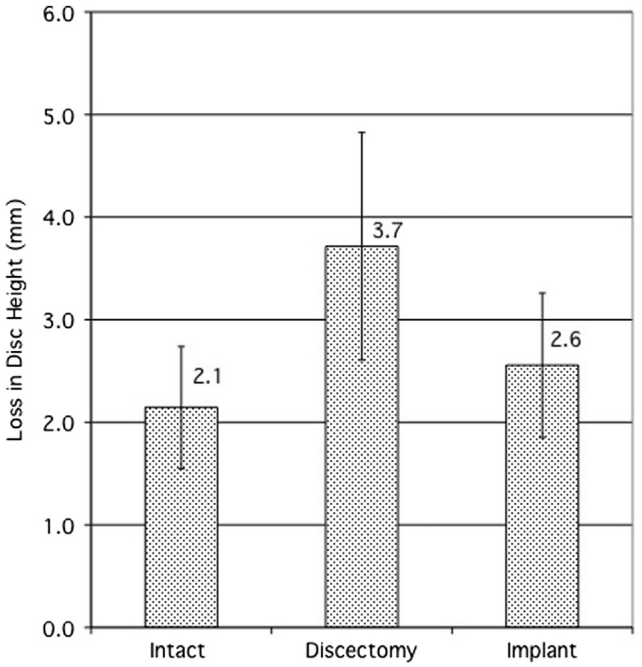

Fig. 5. Mean loss in disc height (mm) at peak compressive load for the 3 disc conditions.

The ROM was analyzed for bending test modes (flexion and extension and left and right bending) at 7.5 Nm on the fifth cycle. Table 3 lists the mean ROM split by level (surgical or control) for the various disc conditions. The control levels displayed consistent motion for all modes throughout the testing. Although the surgical levels showed increased flexion motion following discectomy, this was not statistically significant. For extension, the motion was significantly reduced ($P < .05$) following discectomy. However, the motion was restored and not significantly different from intact status following insertion of the implant. There were no significant changes in left or right bending after discectomy or following insertion of the implant.

The stiffness was measured between 0.8 and 1.2 kN for pure compression, 4.5–7.5 Nm for left and right torsion, flexion and extension, and left and right bending. The data were averaged over the last 3 cycles for each test. Table 4 lists the mean stiffness for pure compression and torsion for each disc condition. There were no significant changes in stiffness for either of these test modes based on condition. Table 5 lists the mean stiffness split by level (surgical or

Table 2
Mean ROM values (degrees) for the torsion test mode in the conditions tested

Mode	Intact	Discectomy	Implant
Left torsion	2.46 ± 0.54	2.75 ± 0.29	2.62 ± 0.42
Right torsion	2.50 ± 0.51	2.80 ± 0.27	2.61 ± 0.38

Table 3
Mean ROM values (degrees) for the sagittal and coronal bending test modes in the conditions tested

Mode	Level	Intact	Discectomy	Implant
Flexion	Control	3.59 ± 0.61	3.67 ± 0.54	3.42 ± 0.60
	Surgical	3.51 ± 0.80	4.55 ± 1.57	4.07 ± 1.66
Extension	Control	2.44 ± 1.17	2.34 ± 1.14	2.33 ± 1.28
	Surgical	2.77 ± 1.14	1.80 ± 0.81*	2.59 ± 0.98
Left bend	Control	2.73 ± 0.70	2.67 ± 0.69	2.71 ± 0.68
	Surgical	3.42 ± 0.99	3.35 ± 1.21	3.04 ± 1.11
Right bend	Control	2.64 ± 0.74	2.65 ± 0.79	2.64 ± 0.80
	Surgical	3.20 ± 0.95	3.49 ± 1.09	3.78 ± 1.46

*Denotes significant difference ($P < .05$) from intact.

control) for the sagittal and coronal bending test modes. The only significant stiffness change was in the extension test mode on the surgical levels. Following discectomy, there was a significant increase ($P < .05$) in stiffness in comparison with the intact condition. With the implant in place, the stiffness was restored and was not significantly different from the intact condition.

Fatigue test

Of the 6 specimens, 5 completed 100,000 cycles of left lateral bend fatigue testing. One specimen did not complete the testing and had to be stopped owing to a specimen failure (disc/endplate separation from the vertebra at the intact level). All implants completed the testing without any extrusions or dislocations. Based on the radiographic images obtained after fatigue testing, there was evidence of an implant shift toward the right lateral annulus. Postfatigue testing radiographs, as well as dissection of the surgical levels, showed no evidence of macroscopic trabecular or endplate fractures. In addition, dissection showed no macroscopic differences between the endplates of the control and surgical levels. Table 1 lists the mean values for intervertebral disc area, width, depth, and the ratio of implant to disc area.

The micro-CT images from the L1 and L4 vertebrae from each test specimen were visually inspected for patterns of microfractures in the trabecula. No visual differences were noted when comparing the areas closest to the control endplate or the endplate closest to the implant. Of the specimens, 4 were noted to be osteopenic. For one of the L1 vertebra, the superior and inferior endplates were noted to have a fracture, but in the opinion of the radiologist, it was considered to be chronic in nature given the intact cortex (Fig. 6). In another L1 vertebra, the superior endplate, which was part of a control level, was noted to have an endplate fracture (Fig. 7) but was also considered to be chronic in nature.

Table 4
Mean stiffness values for the pure compression and torsion test modes in the conditions tested

Mode	Intact	Discectomy	Implant
Pure comp (N/mm)	1485 ± 229	1364 ± 235	1362 ± 241
Left torsion (Nmm/degree)	4056 ± 600	3610 ± 425	3848 ± 316
Right torsion (Nmm/degree)	3696 ± 493	3259 ± 243	3518 ± 278

Discussion

The objective of this study was to initially assess the biomechanical function of an articulating nucleus replacement device in an in vitro cadaveric model and then primarily examine any adverse effects on the intervertebral disc and vertebral endplate under fatigue-loading conditions. Although it appears that there are similarities between this device and the Fernstrom stainless steel ball, ie, both having articulation to facilitate the angulation movement of the disc, there are 2 fundamental differences between them. First, the articulation for the stainless steel ball occurs at the interface between the device and the endplates, whereas this occurs within the device for NUBAC. By changing the articulation interface between the device and endplates, the design of NUBAC reduces the risk of endplate erosion in comparison with the stainless steel ball because of the modulus mismatch of the hard metal surface of the steel ball and the relatively soft vertebral endplates. Second, more importantly, the design of the stainless steel ball has a point contact between the device and the endplates, which leads to high contact stress and therefore a high risk of subsidence. This high subsidence was one of the major failure modes for the stainless steel ball as evidenced by the clinical data. To address this, the design of the PEEK nucleus replacement allows a large contact area between the device and the endplates, and therefore it would reduce the relative stress for a given load and, therefore, the subsidence risk significantly. To achieve the objective of this pilot study, cadaveric lumbar spine specimens underwent simulated surgical procedures and nondestructive biomechanical testing.

Although a cadaveric study can provide useful information to understand the biomechanical behavior of a human spine segment under various pathological conditions or after different surgical treatments, it can also have some inherent limitations. The focus of this study was on the biomechanical behavior of normal and treated spine segment under fatigue-loading conditions and, therefore, used a 2 FSU

Table 5
Mean stiffness values (N = 6) for the sagittal and coronal bending test modes (Nmm/degree)

Mode	Level	Intact	Discectomy	Implant
Flexion	Control	4168 ± 566	3804 ± 360	4034 ± 627
	Surgical	4785 ± 1437	4817 ± 1220	4911 ± 1432
Extension	Control	6032 ± 2148	6754 ± 2220	5983 ± 1640
	Surgical	4759 ± 2441	8925 ± 5397*	5904 ± 2632
Left bend	Control	4557 ± 1214	4578 ± 1294	4522 ± 1283
	Surgical	3566 ± 869	4191 ± 1098	4594 ± 1092
Right bend	Control	4764 ± 1658	4738 ± 1720	4731 ± 1711
	Surgical	3923 ± 1260	4310 ± 1150	4006 ± 1097

*Denotes significant difference ($P < .05$) from intact.

model (contiguous levels) with a control and treated level within the same specimen. Although the biomechanics of the adjacent levels can behave differently under quasi-static testing conditions, we felt this was a more appropriate model under the fatigue-loading conditions in comparison with testing individual FSUs. It is also important to note that only 1 mode of fatigue loading (left lateral bend) was performed and the spine specimens were not tested under extreme-loading conditions. Other fatigue studies on the lumbar spine have focused on flexion loading only and have shown ligamentous effects from 10(k) cycles or less.[27,28] One of the drawbacks of this testing protocol was the amount of time and subsequent potential for specimen deterioration. One of the 6 specimens experienced a ligamentous failure and there were most likely intervertebral disc and ligamentous changes in the other specimens similar to previous studies. Despite the limitations, the model was effective to evaluate a potential extrusion scenario and 5 of the 6 specimens were successfully tested to 100(k) cycles.

The nondestructive biomechanical tests depicted a number of changes for the 2-segment model tested. Following discectomy, there was a significant decrease in the overall axial displacement of the construct in comparison with the intact condition. Although the disc height of the individual segment levels (control and surgical) of each construct was not quantified, the change can be attributed to the surgical level. Previous studies on single-segment models have shown similar results.[29] The other significant changes following discectomy versus the intact condition occurred in the extension ROM and stiffness of the surgical level. After discectomy, there was a reduction in the extension ROM and an increase in stiffness. The changes at the surgical level did not correspond with the changes at the control level for any of the parameters measured.

Insertion of the nucleus implant significantly increased the construct height under load in comparison with the discectomy condition. One of the 6 specimens had an increase in construct height larger than the intact condition. All other implants restored construct height between 49% and 89% of the intact condition. Increasing the disc height at the surgical level is important for sustaining biomechanical characteristics of the intervertebral disc. No significant differences for extension ROM or stiffness existed between the intact and implanted conditions.

Fatigue testing to 100,000 cycles under 2.5–7.5 Nm of load in left lateral bend resulted in no extrusions or dislocations of the implant. Examination of the endplates following gross dissection revealed no visible fractures or differences between the surgical and control levels. In addition, comparing the trabecular bone within the vertebrae adjacent with the endplates showed no fracture patterns or regional differences between the surgical and control levels. The small superior and inferior endplate disruptions with intact cortex, noted in some of the specimens, were

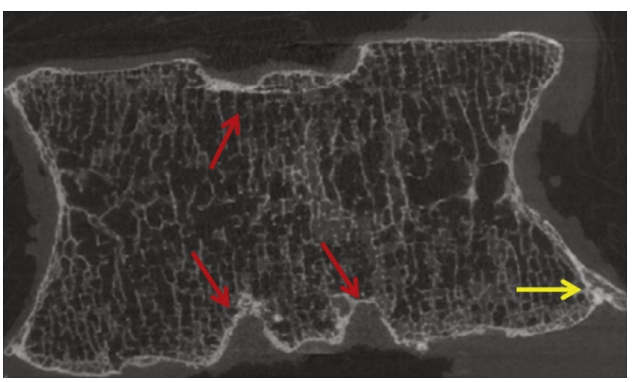

Fig. 6. CT slice of an L1 vertebra. There are superior and inferior endplate fractures (shown by red arrows), all of which are likely to be chronic given the intact cortex. Notice the small osteophytes (yellow arrow) at the inferior endplate. A 3D reconstruction (not shown) confirmed these observations.

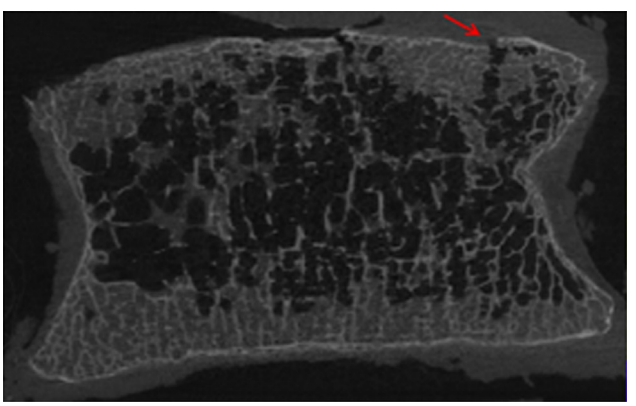

Fig. 7. CT slice of a L1 vertebra. Fracture of the endplate (shown by red arrow) at the control level.

thought to be representative of small, chronic fractures of the endplates associated with DDD. Four of the specimens were considered osteopenic; and, for those that had endplate disruptions, there were small osteophytes noted around the endplates. Unfortunately, because of geometric size restrictions for the scanner, the vertebrae could not be micro-CT scanned before testing to better assess the noted bony changes.

Gross dissection following fatigue testing did show slight migration of the implant in a right lateral direction. The amount of motion could not be quantified without improvements to implant recognition under fluoroscopy. The small amount of migration was not unexpected considering the smooth surface of the interface between the implant and the vertebral endplates. In addition, there was no fixation between the implant and adjacent bone. It should be noted that the unilateral bending fatigue load applied in this study was chosen to represent the worst-case scenario for implant extrusion and does not represent the loading mode of normal daily activities.

Maintaining the maximum flexibility and ROM provided by the implant requires proper alignment of the implant with the joint axis of rotation. Determination of the instantaneous axis of rotation can be complex as it changes with position[30] and degeneration.[31] Having an intervertebral disc implant that is not fixed and allows for small changes in the axis of rotation of the joint is therefore beneficial. In addition, placement of the implant during surgery will be less demanding with regard to optimal location within the joint space in comparison with an implant with fixed endplates.

Conclusion

Similar to what has been reported in the literature, in this study there were disc height losses and biomechanical changes when comparing the after discectomy condition with the intact condition. The disc height loss was restored by the implantation of the nucleus device. There were improvements in ROM and stiffness characteristics with the implant in place compared with the discectomy condition during short-term, quasi-static biomechanical testing. Additionally, in vitro fatigue testing up to 100,000 cycles showed no implant extrusion and no macroscopic changes to the bony structure or cartilaginous endplates when comparing intact and implanted intervertebral discs. A micro-CT evaluation also resulted in no recognizable patterns of bony fracture at the endplates or within the trabecula adjacent to the endplate closest to the nucleus implant.

References

1. Brodke D, Ritter S. Nonsurgical management of low back pain and lumbar disk degeneration. *Instr Course Lect* 2005;54:279–86.
2. Nordin M, Frankel V, Lindh M. Biomechanics of the lumbar spine. Basic Biomechanics of the Musculoskeletal System, 2nd ed, 1989: 183-207.
3. Bao Q, McCullen G, Higham P. The artificial disc: Theory, design and materials. *Biomaterials* 1996;17:1157–67.
4. Markolf KL, Morris JM. The structural components of the intervertebral disc. A study of their contributions to the ability of the disc to withstand compressive forces. *J Bone Joint Surg Am* 1974;56:675–87.
5. Nachemson A. The load on lumbar disks in different positions of the body. *Clin Orthop Relat Res* 1966;45:107–22.
6. Edwards WT, Ordway NR, Zheng Y, et al. Peak stresses observed in the posterior lateral anulus. *Spine (Phila Pa 1976)* 2001;26:1753–9.
7. Loupasis GA, Stamos K, Katonis PG, et al. Seven- to 20-year outcome of lumbar discectomy. *Spine* 1999;24:2313–7.
8. Osterman H, Sund R, Seitsalo S, et al. Risk of multiple reoperations after lumbar discectomy: A population-based study. *Spine* 2003;28: 621–7.
9. Weinstein JN, Lurie JD, Tosteson TD, et al. Surgical vs nonoperative treatment for lumbar disk herniation: The Spine Patient Outcomes Research Trial (SPORT) observational cohort. *J Am Med Assoc* 2006;296:2451–9.
10. Weinstein JN, Lurie JD, Tosteson TD, et al. Surgical versus nonoperative treatment for lumbar disc herniation: four-year results for the Spine Patient Outcomes Research Trial (SPORT). *Spine* 2008;33: 2789–800.
11. Bono CM, Lee CK. Critical analysis of trends in fusion for degenerative disc disease over the past 20 years: Influence of technique on fusion rate and clinical outcome. *Spine* 2004;29:455–63.
12. Bono CM, Lee CK. The influence of subdiagnosis on radiographic and clinical outcomes after lumbar fusion for degenerative disc disorders: An analysis of the literature from two decades. *Spine* 2005;30:227–34.
13. Ghiselli G, Wang JC, Bhatia NN, et al. Adjacent segment degeneration in the lumbar spine. *J Bone Joint Surg Am* 2004(86-A):1497–503.
14. Ghiselli G, Wang JC, Hsu WK, et al. L5-S1 segment survivorship and clinical outcome analysis after L4-L5 isolated fusion. *Spine* 2003;28: 1275–80.
15. Fernstrom U. Arthroplasty with intercorporal endoprothesis in herniated disc and in painful disc. *Acta Chir Scand Suppl* 1966;357:154–9.
16. Mckenzie AH. Fernstrom intervertebral disc arthroplasty: A longterm evaluation. *Ortho Int Ed* 1995;3:313–24.
17. Bao QB, Yuan HA. New technologies in spine: Nucleus replacement. *Spine* 2002;27:1245–7.
18. Ahrens M, Tsantrizos A, Donkersloot P, et al. Nucleus replacement with the DASCOR disc arthroplasty device: Interim two-year efficacy and safety results from two prospective, non-randomized multicenter European studies. *Spine* 2009;34:1376–84.
19. Berlemann U, Schwarzenbach O. An injectable nucleus replacement as an adjunct to microdiscectomy: 2 Year follow-up in a pilot clinical study. *Eur Spine J* 2009;18:1706–12.
20. Bertagnoli R, Sabatino CT, Edwards JT, et al. Mechanical testing of a novel hydrogel nucleus replacement implant. *Spine J* 2005;5:672–81.
21. Bertagnoli R, Schonmayr R. Surgical and clinical results with the PDN prosthetic disc-nucleus device. *Eur Spine J* 2002;11(Suppl 2):S143–8.
22. Allen MJ, Schoonmaker JE, Bauer TW, et al. Preclinical evaluation of a poly (vinyl alcohol) hydrogel implant as a replacement for the nucleus pulposus. *Spine* 2004;29:515–23.
23. Jin D, Qu D, Zhao L, et al. Prosthetic disc nucleus (PDN) replacement for lumbar disc herniation: Preliminary report with six months' follow-up. *J Spinal Disord Tech* 2003;16:331–7.
24. Shim CS, Lee SH, Park CW, et al. Partial disc replacement with the PDN prosthetic disc nucleus device: Early clinical results. *J Spinal Disord Tech* 2003;16:324–30.
25. Brown T, Bao QB, Kilpela T, et al. An in vitro biotribological assessment of NUBAC, a polyetheretherketone-on-polyetheretherketone articulating nucleus replacement device: Methodology and results from a series of

wear tests using different motion profiles, test frequencies, and environmental conditions. *Spine* 2010;35:E774–81.
26. Lee JL, Billi F, Sangiorgio SN, et al. Wear of an experimental metal-on-metal artificial disc for the lumbar spine. *Spine* 2008;33:597–606.
27. Adams MA, Hutton WC. The effect of fatigue on the lumbar intervertebral disc. *J Bone Joint Surg Br* 1983;65:199–203.
28. Goel VK, Voo LM, Weinstein JN, et al. Response of the ligamentous lumbar spine to cyclic bending loads. *Spine* 1988;13:294–300.
29. Goel VK, Goyal S, Clark C, et al. Kinematics of the whole lumbar spine. Effect of discectomy. *Spine (Phila Pa 1976)* 1985;10:543–54.
30. Gertzbein SD, Holtby R, Tile M, et al. Determination of a locus of instantaneous centers of rotation of the lumbar disc by moire fringes. A new technique. *Spine* 1984;9:409–13.
31. Gertzbein SD, Seligman J, Holtby R, et al. Centrode patterns and segmental instability in degenerative disc disease. *Spine* 1985;10:257–61.